PERGAMON

Microelectronics Reliability 41 (2001) 1519–1524

MICROELECTRONICS RELIABILITY

www.elsevier.com/locate/microrel

Analysis of high-power devices using proton beam induced charge microscopy

M. Zmeck[a,b,c], J. Phang[a], A. Bettiol[b], T. Osipowicz[b], F. Watt[b], L. Balk[c], F.-J. Niedernostheide[d], H.-J. Schulze[d], E. Falck[e], R. Barthelmess[e]

[a]*Centre for Integrated Circuit Failure Analysis and Reliability, National University of Singapore, Singapore,*
[b]*Research Centre for Nuclear Microscopy, National University of Singapore, Singapore,*
[c]*Lehrstuhl für Elektronik, Universität Wuppertal, Germany,*
[d]*Infineon AG, München, Germany,*
[e]*eupec, Warstein, Germany*

Abstract

Ion beam induced charge microscopy (IBIC microscopy) has been used for several years to analyse various types of semiconductor devices [1]. In this paper the potential of IBIC-microscopy for the analysis of deeply buried structures of high power devices is discussed. The advantages of the analysis of charge collection spectra taken under reverse voltages (at around 10% of the design value) are discussed. In this work a high-voltage diode with a field ring structure has been analysed using a 2 MeV proton beam applying bias voltages up to 500 V.
© 2001 Elsevier Science Ltd. All rights reserved.

1. Introduction:

The necessary conditions that have to be met in order to achieve uniform current distributions and high breakdown voltages in high-power devices are large depletion regions and highly homogeneous doping levels. Hence analytical techniques able to reach such deeply located structures of high power devices are necessary. IBIC-microscopy is a powerful tool for such analyses. The technique has been used in a previous study for the analysis of 8 kV light-triggered thyristors [2]. The application of a reverse bias voltage allows one to obtain information about the field distribution within the device under working conditions. Such data will help in the design process of high power devices so that excessive fields can be avoided, for example at device edge regions. A further aspect in using IBIC-microscopy is the consideration of effects stemming from cosmic radiation [3]. With increasing field strength the sensitivity to cosmic radiation increases for most devices. Therefore it is important to keep the field strength below a certain level, and it is intriguing to check such conditions with the IBIC technique.

The 2 MeV proton beam used for the analysis has a range of about 47 μm and a lateral straggling of about 3 μm near the end of range, a much smaller value than that of an electron beam of the same range. This enables a much higher spatial resolution if deep, buried *p-n* junctions have to be analysed [4]. Since the ion beam creates considerable damage it is necessary to keep the ion dose low.

2. Experimental setup

The structure of the high-voltage diode investigated is sketched in figure 1. The depth of the p^+-regions of the main diode and field rings is about 30 μm. The field ring structure of the investigated diode was terminated with a especially developed a-C:H passivation [5].

0026-2714/01/$ - see front matter © 2001 Elsevier Science Ltd. All rights reserved.
PII: S0026-2714(01)00159-7

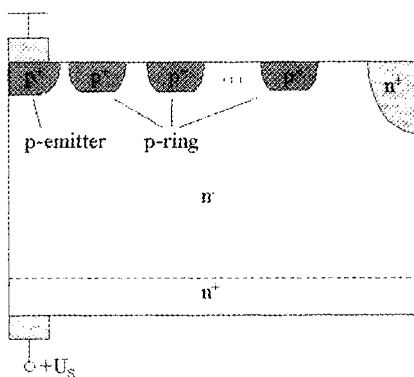

Fig. 1. Schematic drawing of the field ring structure of the high voltage diode

The measurements are carried out at the new nuclear microprobe facility, Research Centre for Nuclear Microscopy, National University of Singapore. A 3.5 MeV singletron accelerator supplies the 2 MeV proton beam.

In figure 2 the measure circuit used for the experiments is depicted. The beam is focused and scanned using the Om2000 endstage [2]. In all experiments the sample was adjusted such that the ions penetrate into the diode from its upper side (anode side). The high-power devices analysed exhibit a relatively low ohmic resistance when compared to the surface barrier detectors typically used for ion beam

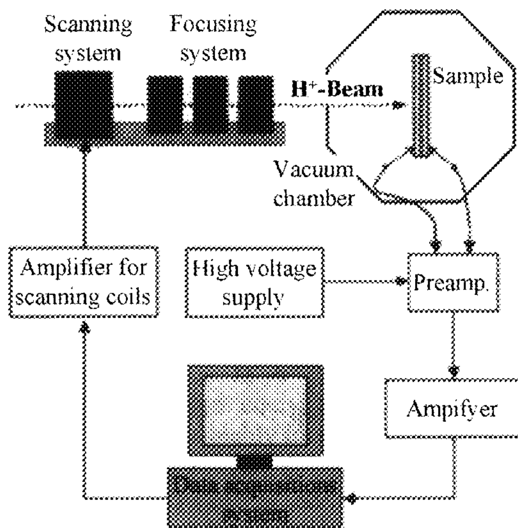

Fig. 2. Measure circuit used

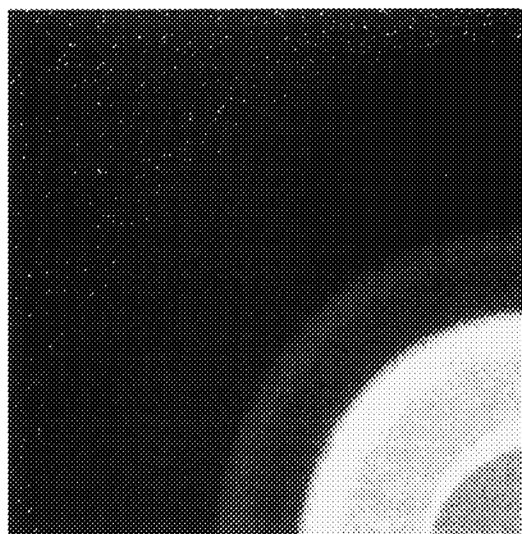

Fig. 3. Median value image of one of the device edges. The first three of eight field rings are shown by the different contrasts. The area shown has a size of about 1 mm^2.

analysis, therefore the preamplifier (Canberra 2003BT) was modified by changing the high-voltage input resistor. This is important in order to keep the voltage drop within the preamplifier small. The bias high voltage was delivered by a Fug HCN 14-6500 high voltage supply.

3. Results:

3.1. IBIC spectra

The IBIC image of an edge of the investigated high-voltage diode is shown in figure 3. For this measurement a reverse bias voltage of 500 V has been applied between the anode and the cathode of the device. The ion dose for this image was less than 2 ions per μm^{-2}. Analysis of the data has shown that ion doses of 1 μm^{-2} are sufficient to obtain images of comparably high resolution.

Additional information can be gained from the charge spectra generated from the experimental data. These spectra show the number of events for a given charge collection window. Using these spectra certain regions (windows) can be defined in the spectrum in order to generate spatial resolved images of the count rates for the measured values within the defined region. The different peaks of the spectra are representing

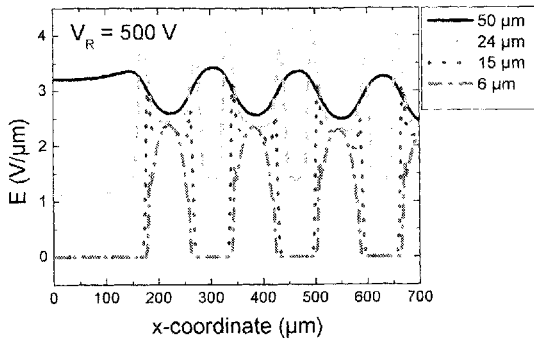

Fig. 4. Electric field distribution in the field ring structure near the p-emitter of the diode at different depths from the semiconductor surface at a reverse voltage of 500 V.

individual features of the device. If these peaks are defined as windows, images can be generated showing the spatial distribution of these individual features.

In the charge collection spectrum from the diode (figure 5, top) a number of peaks are clearly visible. The 9 images below the spectrum in figure 5 are generated from the grey marked regions of the spectrum. Regions of a specific brightness represent areas of a specific charge collection efficiency, i.e. structurally different regions. This shows that the mapping of individual peaks in the charge collection spectra reveals the geometry of individual, structurally different device regions.

In order to calculate the electrical field distribution inside the diode taking into account the influence of this junction termination the Poisson solver BREAKDOWN was used. Figure 4 shows the electric field profiles at 4 different depths. Obviously, there is a distinct correlation between signals in the IBIC-image and the regions with locally increased electric fields. For example, the broad rings in the spectrum 1, 2, 3, and 7 correspond to the three inner p-rings and a part of the p-emitter, respectively (cf. Fig. 1). The centres of the three rings correspond to the local field maxima at a depth of about 50 µm. The thin outer rings in the spectra 3, 4 and 8 coincide with the local field maxima in a depth of 6 µm. The two rings visible in spectrum 5 can be attributed to field maxima surrounding the innermost p-ring in a depth of about 24 µm. However, the exact position of the local field maxima vary with the depth, as obvious from the field distributions at a depth of 24 and 15 µm. A corresponding shift is also visible from spectrum 4 (two inner rings) to spectrum 5.

Attention should be paid to the influence of the generated charge along the hole penetration path of the ions complicating the correlation of the IBIC signals to a specific depth considered in the simulation calculation.

3.2. *Influence of increasing bias voltages*

In figure 6 the median value images and their spectra using different bias conditions are compared. The images show the region just near the emitter metalization towards to the device edge.

The IBIC image in figure 6 a) was generated without bias voltage. Only the p^+-emitter region shows large contrast. Therefore only a single peak appears in the charge spectrum.

The signal to noise level present in the IBIC images is obviously improved by the application of a bias voltage of 140 V as shown in figure 6 b), clearly the contours present in the image are much sharper. In the spectrum of this image the peaks have moved to higher charge collection efficiency regions. Because of the reverse bias voltage the lateral depletion region of the main pn-junction spreads further into the depth and covers almost the whole dissipation volume of the ion beam, leading to an increase of the charge collection efficiency.

With a further increase of the bias voltage the depletion regions spread laterally and also further into the depth of the device. In the case of figure 6 c) the first field rings are becoming visible in the IBIC image for a bias voltage of 260 V. New individual peaks in the low charge region of the spectrum characterize these further features of the device.

Using a bias voltage of 440 V, again more structures are appearing in the IBIC images shown in figure 6 d). The new peaks visible in the previous spectra have moved to the higher charge collection regions of the spectrum, but the certain other peaks have kept their position. This demonstrates a saturation effect that occurs if the depth of the depletion region substantially exceeds the range of the ion beam. In this limit the depletion region collects nearly all of the induced charges.

4. Conclusion and Outlook:

It has been shown that valuable information concerning the internal field distribution inside high-power diodes under working conditions can be

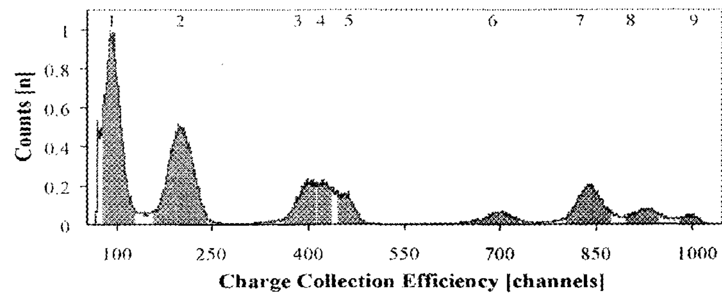

Fig. 5. Charge spectrum (top) of the diode at a reverse voltage of 500 V; the 9 images show the spatial distributed count rates of the grey marked regions in the spectrum. The area shown is the same as in Fig. 3.

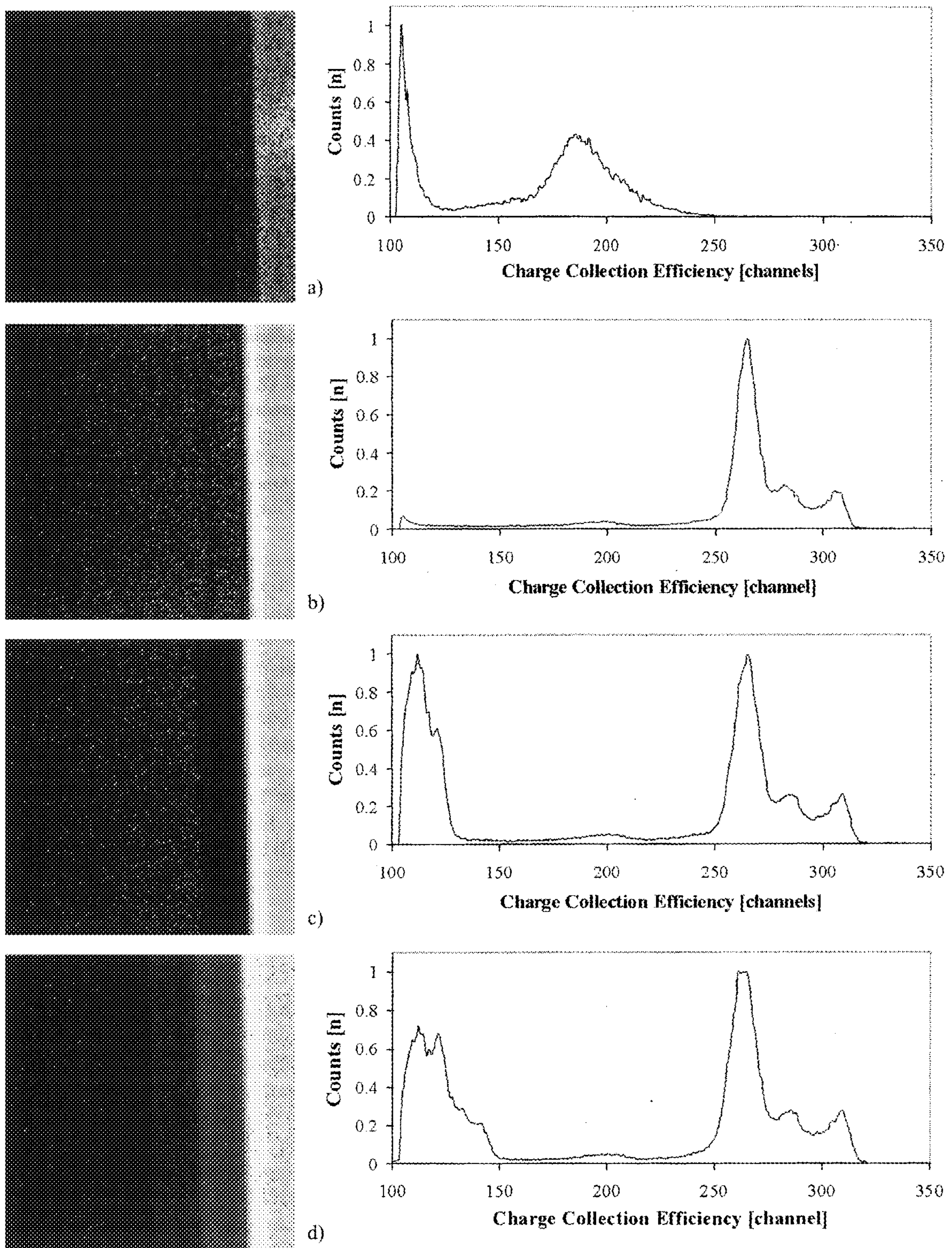

Fig. 6: Median value images and their spectra for different bias voltages: a) no bias, b) 140 V, c) 260 V and d) 440 V.

obtained by evaluating IBIC-images in combination with the charge spectrum. Therefore, IBIC microscopy is a promising tool to optimise the field distribution in high-power devices.

In order to get a more detailed understanding of the IBIC-images and spectra, experiments are under way using different proton energies. Different energies are selected and the charge collection efficiency is measured via IBIC. The results will be compared with field simulation calculations at a depth equivalent to the ion beam range. Using these data, models will be deduced enabling a quantitative analysis of the device structures.

References:

[1] Schöne H., Jamieson D. N., Bulletin, A Publication of the Materials Research Society 25 (2000), pp. 14-20

[2] Zmeck M., Osipowicz T., Watt F., Niedernostheide F.-J., Schulze H.-J., Fiege G.B.M., Balk L., Analysis of High-Power Devices Using Proton Beam Induced Currents, Microelectron. Reliab. 49 (2000), pp. 1413-1418

[3] Voss, P., Maier, K.H., Meczynski, W., Becker, H.W., Normand, E., Wert, J.L., Oberg, D.I., Majewski, P.P., Irradiation experiments with high-voltage power devices as a possible means to predict failure rates due to cosmic rays, Proceedings of 9th International Symposium on Power Semiconductor Devices and IC's (1997), pp. 169.

[4] Breese M. B. H., Jamieson D. N., King P. J. C., Materials Analyses Using A Nuclear Microprobe, John Wiley & Sons, Inc. (1996)

[5] Barthelmeß R., Beuermann M., Metzner D., Schmidt G., Westerholt D., Winter N., Gerstenmaier Y.C., Reznik D., Ruff M., Schulze H.-J., and Willmeroth A., "Electroactive Passivation of High Power Semiconductor Devices with Punch Through Design by Hydrogenated Amorphous Carbon Layers (a-C:H)", Proc. of the ISPSD (1998), pp. 181-184